Brazil-Malvinas confluence: effects of environmental variability on phytoplankton community structure

RAFAEL GONÇALVES-ARAUJO[1]*, MÁRCIO SILVA DE SOUZA[1], CARLOS RAFAEL BORGES MENDES[1,2], VIRGINIA MARIA TAVANO[1], RICARDO CESAR POLLERY[3] AND CARLOS ALBERTO EIRAS GARCIA[1]

[1]INSTITUTO DE OCEANOGRAFIA (FURG), PO BOX 474, CAMPUS CARREIROS, RIO GRANDE 96201-900, BRAZIL, [2]FACULDADE DE CIÈNCIAS, CENTRO DE OCEANOGRAFIA, UNIVERSIDADE DE LISBOA, CAMPO GRANDE, LISBON 1749-016, PORTUGAL AND [3]LABORATÓRIO DE BIOGEOQUÍMICA, DEPARTAMENTO DE ECOLOGIA, INSTITUTO DE BIOLOGIA (UFRJ), CIDADE UNIVERSITÁRIA, RIO DE JANEIRO 21941-590, BRAZIL

*CORRESPONDING AUTHOR: rafaelgoncalvesaraujo@gmail.com

This study investigates the relationships between the spring phytoplankton community and environmental factors in the Brazil-Malvinas confluence region. Phytoplankton community composition was determined by the high performance liquid chromatography/CHEMTAX approach, complemented with microscopic examination. Abiotic factors included temperature, salinity, dissolved inorganic macronutrients (ammonium, nitrite, nitrate, phosphate and silicate), water column stability and upper mixed layer depth (UMLD). These environmental variables were reasonably informative to explain the variability of the phytoplankton communities (44% of variation explained). Cluster and canonical correspondence analyses allowed discrimination of four zones (coastal, Sub-Antarctic, tropical and intermediate zones), also identifiable in the T−S diagrams and in the nutrient spatial distribution patterns. The presence of nutrient-rich Sub-Antarctic waters was a major oceanographic feature, associated with diatoms and dinoflagellates. However, in the Sub-Antarctic zone, biomass was particularly low, probably as a result of grazing pressure, as suggested by chemical and biological indicators. In contrast, in oligotrophic tropical waters, phytoplankton was mainly composed by small nanoflagellates and cyanobacteria. A large intermediate zone was also dominated by nanoflagellates, mainly *Phaeocystis antarctica*, probably favored by strong water column stability. The coastal zone exhibited fairly similar conditions to those in the intermediate zone, but with deeper UMLD, a favorable condition for diatom growth. These results emphasize the importance of the properties of water masses and also biological processes such as grazing in structuring phytoplankton communities in the region.

KEYWORDS: Brazil-Malvinas confluence; physical structure; nutrients; phytoplankton; HPLC-CHEMTAX

INTRODUCTION

The Brazil-Malvinas confluence (BMC) region (Fig. 1) is located ~38°S in the southwestern Atlantic Ocean, encompassing mainly a pelagic domain with dynamic interaction between the Brazil current (BC) and Malvinas current (MC) (Gordon, 1989; Chelton *et al.*,
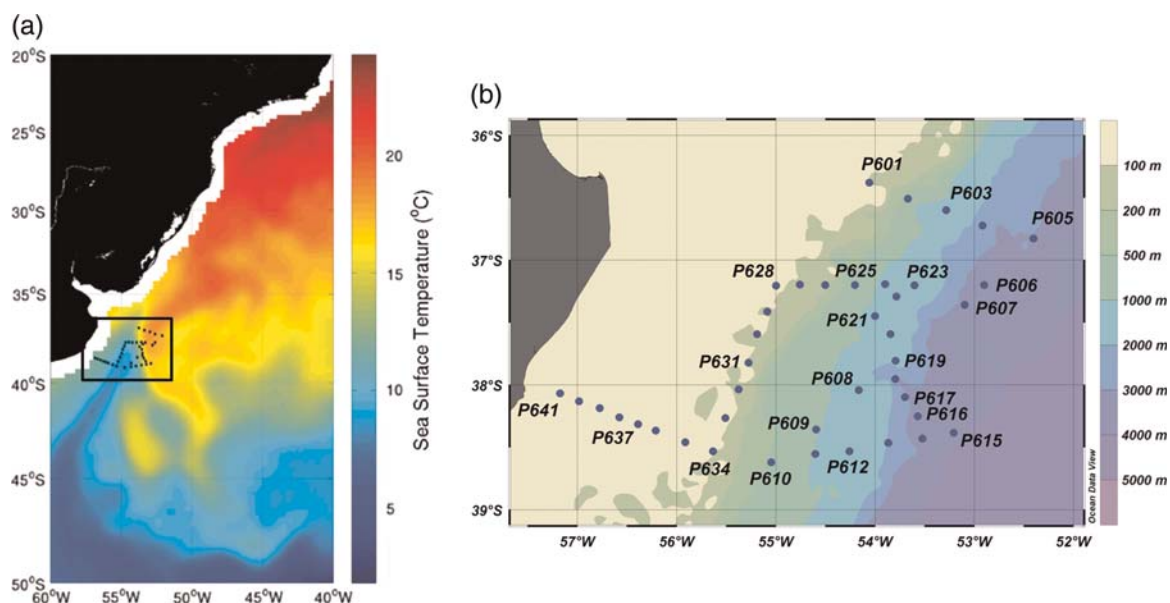
Fig. 1. AMSR-E 8-day sea surface temperature (SST) (°C) composite map for 11–17 October 2008, showing the location of 41 oceanographic stations occupied at the Brazil-Malvinas confluence region during the 'PATEX VI' cruise (**a**) and a detailed map (**b**) showing some station labels over the cruise track.

1990). These currents flow in opposite directions and their mixing generates a marked thermohaline frontal zone (Peterson and Stramma, 1991; Souza and Robinson, 2004; Pezzi et al., 2009) recognized as one of the most energetic in the world's oceans (Gordon, 1989). The BC is generated near 10°S and flows southwards carrying tropical waters (TW) with high temperature (>26°C) and salinity (between 34.0 and 36.7) (Stramma and England, 1999). The northward MC is formed by a ramification of the Antarctic Circumpolar Current (ACC) due to topographic effects (Matano, 1993) and transports Sub-Antarctic waters (SAW) with surface temperatures <10°C in the austral winter and salinity values <34.3 (Bianchi et al., 2002).

Although there have been a large number of studies carried out within the BMC region (e.g. Provost et al., 1996; Bianchi et al., 2002; Pezzi et al., 2005; Matano et al., 2010), only a few have been concerned with the distribution of phytoplankton assemblages and their association with environmental factors (e.g. Gayoso and Podestá, 1996; Fernandes and Brandini, 1999; Brandini et al., 2000; Olguín et al., 2006; Painter et al., 2010). Based on analysis of in situ data, it has been shown that the BMC is an area of enhanced chlorophyll a (Chl a) concentration promoted by the contrasting characteristics of the two currents, allowing phytoplankton growth in the surface layers (Brandini et al., 2000). This enhancement can stimulate the development of subsequent food web trophic levels in the BMC region, from copepods to elephant seals (Berasategui et al., 2005; Campagna et al., 2006).

Some studies in the region have reported distribution patterns of phytoplankton communities and biomass either at spatial or temporal scales. For instance, distinct zones have been recognized in the BMC region based on Chl a levels (Carreto et al., 1995) and specific phytoplankton groups were shown to be associated with particular hydrographic features along cross-shelf sections between the Río de La Plata and the oceanic waters of the subtropical convergence (Carreto et al., 2008). These authors have identified a Phaeocystis sp. dominated community associated to the MC, while another report has described an assemblage composed mainly of diatoms and dinoflagellates at the shelf-break, under the influence of SAWs (Garcia et al., 2008). Different haptophyte populations have also been described in the SW Atlantic, by using a chemical taxonomic approach derived from pigment data. These were associated with particular hydrographic features of the BMC and the outer estuary of Río de La Plata: Haptophytes B (represented by Emiliania spp. and Chrysochromulina spp.) were associated to coastal waters; Haptophytes C (mainly the coccolithophorid Emiliania huxleyi) were linked to the continental shelf domain; Haptophytes D (mainly Phaeocystis antarctica) were more related to the cold waters of MC and Haptophytes E (composed by other coccolithophorid species) predominated within the BC domain (Carreto et al., 2003). Thus, the diverse physical

environments associated with the BMC at both spatial and time scales influence the development of distinct phytoplankton assemblages, which, in turn, can influence the trophic web structure in the region.

This study aims to investigate the relationship between physical and chemical parameters and the spatial distribution of the phytoplankton community in the BMC region, using the high performance liquid chromatography (HPLC)-CHEMTAX approach as well as microscopic phytoplankton analysis.

METHOD

Sampling

Data were collected at 41 oceanographic stations throughout the study area (Fig. 1) visited during the 13–18 October 2008 period onboard the Brazilian Navy RV *Ary Rongel*. The sampling was carried out during the springtime operation of the PATEX (PATagonian EXperiment) program, named 'PATEX VI'. Surface water was sampled using a Van Dorn bottle and water samples from discrete depths were collected using Niskin bottles attached to a combined rosette CTD SeaBird® 911 carrousel system. The instrument was also equipped with an *in vivo* chlorophyll fluorescence sensor (SeaTech fluorometer). The vertical fluorescence profile was used as a guide to select sampling depths for biological and chemical measurements.

Physical parameters

Potential density and stability (*E*) of the water column were calculated using potential temperature and salinity data obtained by CTD casts. Stability is based on vertical density variations, as a function of the buoyancy or Brunt–Väisälä frequency (N^2), which is defined by

$$N^2 = -\frac{g}{\rho}\frac{\partial \rho}{\partial z} \ (\text{rad}^2 \ \text{s}^{-2}) \text{ leading to } E = \frac{N^2}{g} \ (10^{-8} \ \text{rad}^2 \ \text{m}^{-1}),$$

where *g* is gravity and *ρ* is the potential water density. In this study, *E* values in the upper 100 m for all stations occupied were averaged in order to represent the stability of the upper surface layer. Upper mixed layer depth (UMLD) was determined from $\partial\rho/\partial z$ profiles. The depth where variations were >0.05 over a 1 m interval was considered the UMLD (m) [adapted from Mitchell and Holm-Hansen (Mitchell and Holm-Hansen, 1991)]. Classification of water masses was based on an adaptation of the thermohaline intervals used by Möller *et al.* (Möller *et al.*, 2008) and Bianchi *et al.* (Bianchi *et al.*, 2005) (Table I).

Table I: Thermohaline ranges used to characterize water masses in the region

Water mass	Temperature (°C)	Salinity
Tropical water (TW)	≥18.5	>36
Subtropical shelf water (STSW)	>14	33.5 < S < 35.3
	>18.5	35.3 < S < 36
South Atlantic central water (SACW)	≤18.5	≥35.3
Sub-Antarctic shelf water (SASW)	9 < T ≤ 11.5	33.5 ≤ S ≤ 34
Sub-Antarctic water (SAW)	9 ≤ T ≤ 14	33.5 ≤ S ≤ 34.2
Low salinity coastal water (LSCW)	—	<33.5

Adapted from Bianchi *et al.* and Moller *et al.* (Bianchi *et al.*, 2005; Möller *et al.*, 2008).

Nutrient analysis

Water samples for dissolved inorganic nutrient measurements (nitrate, nitrite, ammonium, phosphate and silicate) were filtered on cellulose acetate membrane filters. Nutrients were analyzed on board ship, following the processing recommendations in Aminot and Chaussepied (Aminot and Chaussepied, 1983). Ammonium was measured by the method of Koroleff (Koroleff, 1969) following modifications in Aminot and Chaussepied (Aminot and Chaussepied, 1983) and absorbance readings at 630 nm. Orthophosphate was measured by its reaction with ammonium molybdate and absorption reading at 885 nm. Silicate measurements in the form of reactive Si were corrected for sea salt interference following Aminot and Chaussepied (Aminot and Chaussepied, 1983). Absorbance values for all nutrients were measured in a FEMTO® spectrophotometer.

Phytoplankton pigment analysis

Samples for phytoplankton pigment analysis were collected from the surface and from fluorescence peak depths, at the locations where they could be detected. Sample volumes ranging from 0.5 to 2 L (depending on the concentration of material) were immediately filtered (filtration not longer than 1 h) onto Whatman GF/F filters (nominal pore size 0.7-μm and 25-mm diameter) under vacuum pressure <5 in. Hg, and kept in liquid nitrogen until analysis. Pigment concentrations were determined by HPLC following the procedure in Zapata *et al.* (Zapata *et al.*, 2000) and modifications in Mendes *et al.* (Mendes *et al.*, 2007). Chl *a* concentration data from HPLC analysis were used as a phytoplankton biomass index, since photosynthetic pigment is common to all autotrophic phytoplankton.

CHEMTAX analysis

The relative abundance of microalgal classes contributing to total Chl a biomass was calculated from pigment data using version 1.95 of CHEMTAX software (Mackey et al., 1996). CHEMTAX uses a factor analysis and steepest-descent algorithm to find the best fit of the data on to an initial pigment ratio matrix. The basis of the calculations and procedures used are fully described in Mackey et al. (Mackey et al., 1996).

Based on microscopic observations and diagnostic pigments detected, seven algal groups were loaded into CHEMTAX: diatoms, dinoflagellates-1 [peridinin (Perid)-containing species], 'chemotaxonomic group', 'Phaeocystis antarctica', cryptophytes, prasinophytes and cyanobacteria (Table II). The pigments loaded were alloxanthin (Allo), fucoxanthin (Fuco), Perid, prasinoxanthin (Prasino), zeaxanthin (Zea), 19′-butanoyloxyfucoxanthin (But-fuco), 19′-hexanoyloxyfucoxanthin (Hex-fuco), chlorophyll c_3 (Chl c_3), chlorophyll b (Chl b) and Chl a. The 'chemotaxonomic group' was defined as having a pigment signature including Fuco, But-fuco, Hex-fuco and Chl c_3, relative to a group that includes Perid-lacking autotrophic dinoflagellates (Wright and Jeffrey, 2006) and other algal groups whose pigment composition has not yet been exhaustively analyzed (e.g. Parmales and Chrysophytes).

Initial pigment: Chl a input ratios were derived from the literature (Carreto et al., 2003; de Souza et al., 2011)

(Table II). The same initial ratio matrix was used for both depths (surface and fluorescence peak depth), but data from each layer were run separately. For optimization of input matrices, a series of 60 pigment ratio tables was generated by multiplying each ratio of the initial table by a random function as described in Wright et al. (Wright et al., 2009). The average of the best six output matrices (with the lowest residual root mean square errors) were taken as the optimized results (Table II).

Phytoplankton microscopic analysis

Surface sea water samples were preserved in amber glass flasks (∼250 mL) with 2% alkaline Lugol's iodine solution for phytoplankton counting and identification. Settling chambers with a volume of 50 mL were examined under the inverted microscope (Utermöhl, 1958; Sournia, 1978). Phytoplankton composition was determined with an Axiovert 135 ZEISS microscope, at ×200, ×400 and ×1000 magnification, according to specific literature (mainly, Dodge, 1982; Hasle and Syvertsen, 1996). Identified species (or groups) were classified as Flagellates I (<5 μm) probably including mainly prasinophytes while Flagellates II (5–10 μm) include cryptophytes as well as chrysophytes. Among the dinoflagellates, some genera include several forms

Table II: Output ratios of marker pigment to Chl a for surface and fluorescence peak (FP)

	Allo	Fuco	Perid	Prasino	Zea	But-fuco	Hex-fuco	Chl c_3	Chl b	Chl a
Input matrix										
Diatoms	0	0.863	0	0	0	0	0	0	0	1
Dinoflagellates-1	0	0	0.8	0	0	0	0	0	0	1
Chemotaxonomic group	0	0.313	0	0	0	0.28	0.491	0.243	0	1
Phaeocystis antarctica	0	0.174	0	0	0	0.105	0.396	0.154	0	1
Cryptophytes	0.7	0	0	0	0	0	0	0	0	1
Prasinophytes	0	0	0	0.372	0	0	0	0	1.156	1
Cyanobacteria	0	0	0	0	1.115	0	0	0	0	1
Output matrix (surface)										
Diatoms	0	0.954	0	0	0	0	0	0	0	1
Dinoflagellates-1	0	0	0.704	0	0	0	0	0	0	1
Chemotaxonomic group	0	0.330	0	0	0	0.440	0.613	0.367	0	1
Phaeocystis antarctica	0	0.276	0	0	0	0.098	0.874	0.495	0	1
Cryptophytes	0.458	0	0	0	0	0	0	0	0	1
Prasinophytes	0	0	0	0.111	0	0	0	0	0.806	1
Cyanobacteria	0	0	0	0	0.931	0	0	0	0	1
Output matrix (FP)										
Diatoms	0	1.009	0	0	0	0	0	0	0	1
Dinoflagellates-1	0	0	0.681	0	0	0	0	0	0	1
Chemotaxonomic group	0	0.379	0	0	0	0.283	0.696	0.440	0	1
Phaeocystis antarctica	0	0.477	0	0	0	0.237	0.877	0.615	0	1
Cryptophytes	0.503	0	0	0	0	0	0	0	0	1
Prasinophytes	0	0	0	0.168	0	0	0	0	0.811	1
Cyanobacteria	0	0	0	0	0.913	0	0	0	0	1

Input ratios were obtained from the literature (Carreto et al., 2003; de Souza et al., 2011) and output ratios are according to the procedure in the 'Methods' section.

and were, for instance, represented as *Gymnodinum* spp., *Gyrodinium* spp. and *Protoperidinium* spp. Other dinoflagellates were identified at order level (Peridiniales). When genus or species identification of diatoms was not possible they were grouped at order level (Centrales and/or Pennales). Except for the identification of the autotrophic *Myrionecta rubra*, other ciliates were generally identified at genus level.

Statistical analysis

As more details on phytoplankton composition are provided by microscopy data, multivariate statistics were run based on microscopic analysis.

Cluster analysis using group average linkage and Bray−Curtis similarity index (Clarke and Warwick, 1994) was used to describe the surface spatial distribution abundance of major phytoplankton species (derived from microscopic analysis) over the survey area. The contribution of the more frequent (>10% in all samples) algal category to total abundance at each site was log-transformed to suppress the scale variability (Zar, 1999) and used as input data. Algal categories were combinations of species of the same genus or similar size. Less abundant categories were grouped at higher taxonomic levels.

Canonical correspondence analysis (CCA) was performed in order to identify the main patterns of community and species variability, with respect to environmental variables (Ter Braak and Prentice, 1988). The analysis was carried out in order to corroborate the assumption that the water masses (through their conservative and non-conservative properties) within the region directly influenced the phytoplankton community structure. Biotic variables were represented by abundances of the main phytoplankton taxonomic groups determined from microscopic analysis, except for the contribution of cyanobacteria, which were only identified by CHEMTAX. Environmental variables included surface temperature, salinity, dissolved inorganic nitrogen (DIN: nitrate, nitrite and ammonium), phosphate, silicate, UMLD and stability. All variables were log-transformed before analysis to reduce the influence of the different scales in the sets of analyzed variables. To test the significance of the CCA, Monte-Carlo tests were run based on 499 permutations under a reduced model ($P < 0.05$). Some sampling stations were excluded from the statistical analyses because no chemical data were available (St. P611 and P627); no microscopic observations (St. P602, P604, P638, P640) or no HPLC data (St. P601, P602, P636, P640). The two first significant canonical roots are used to produce the canonical diagram. The canonical roots are the weighted sums of the phytoplankton variables, which are used to calculate the position of the stations in the diagram according to their algal composition and abundance. Thus, the distances between stations in the ordination diagram reflect the degree of similarity among their phytoplankton assemblages (short distances indicate high similarity). Canonical factor loadings are the simple correlations between the environmental variables and the canonical roots, and are considered a measurement of the importance of the different environmental variables determining phytoplankton variability within the area.

RESULTS

Physical setting

Surface distribution of temperature (Fig. 2a) and salinity (Fig. 2b) showed great spatial variability and a thermohaline front over the sampling area. Temperature ranged from 8.1 (St. P611) to 18.8°C (St. P615), displaying a strong horizontal thermal gradient over the shelf-break region, reaching 0.173°C km^{-1} (from St. P613 to St. P615). Salinity ranged from 33.04 (St. P614) to 35.98 (St. P615) (Fig. 2b). A T−S diagram from the upper 100 m (Fig. 3) shows the presence of six water masses (Table I): Sub-Antarctic shelf water (SASW), SAW, TW, sub-tropical shelf water (STSW),
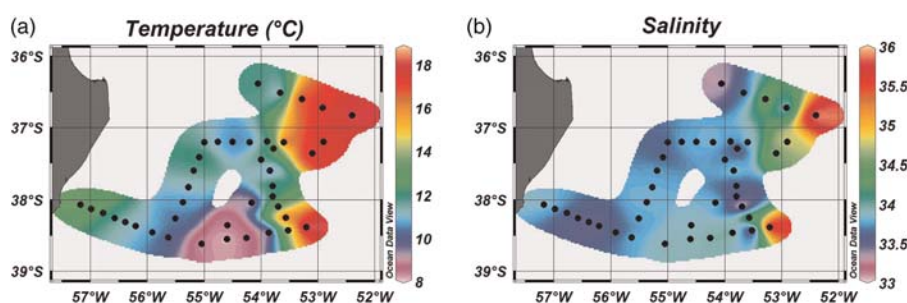

Fig. 2. Surface distributions of temperature (°C) (**a**) and salinity (**b**) over the study area.

south Atlantic central water (SACW) and low salinity coastal water (LSCW) (Fig. 3). Some points in the T–S diagram (Fig. 3) resulted from combinations between water masses and were, therefore, not classified.
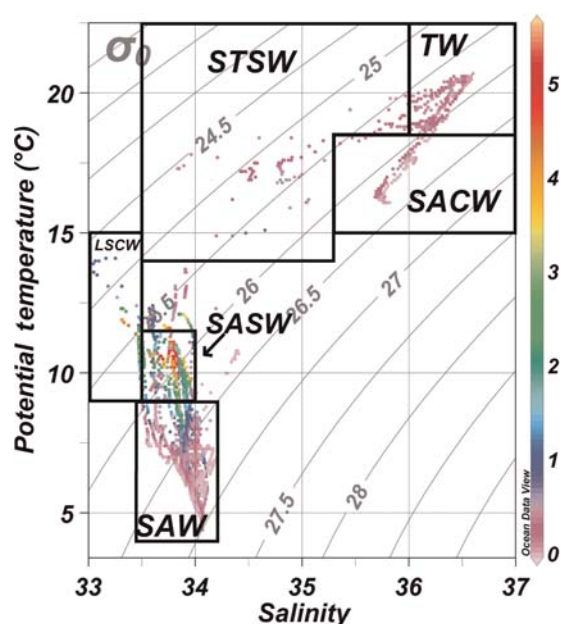

Fig. 3. T–S diagram for the first 100 m of all stations occupied during the 'PATEX VI' cruise. Dotted spaces indicate Chl *a* fluorescence (mg m^{-3} on the color bar). Dots that are not classified as a specific water mass are represented by mixing of SAW and TW. SASW, Sub-Antarctic shelf water; SAW, Sub-Antarctic water; TW, tropical water; STSW, sub-tropical shelf water; SACW, south Atlantic central water; LSCW, low salinity coastal water.

Surface distribution of inorganic nutrients

The highest surface values of DIN (11.62 µM) and phosphate (0.89 µM) concentrations were found at station P611, dominated by SAW (Fig. 4a and b, respectively), while the lowest concentrations (0.94 µM of DIN and 0.18 µM of phosphate) were found at St. P605, under the TW influence (Fig. 4a and b). In addition, phosphate was higher toward coastal stations, reaching 0.79 µM at St. P641 (Fig. 4b). In contrast, silicate levels were higher in the northeastern part of the study area, mainly associated with TW (maximum 7.33 µM at St. P604), and were low at coastal sites, with values up to 3 µM (Fig. 4c). Consequently, the nutrient ratios (N:P and Si:N) showed a distribution pattern that reflected the zonation adopted in this study (Fig. 7). Overall, N:P ratios close to the Redfield-Brzezinski ratio (15Si:16N:1P) were found only when associated with the SAW, whereas values <10 N:P were found throughout the rest of the sampling area (Fig. 4d). Si:N ratios were mostly between 1 and 3, except a higher value at St. P605 in the TW and the particularly low values at the southern area, under SAW influence (Fig. 4e).

Phytoplankton community and chlorophyll *a* distribution

Surface Chl *a* concentration varied between 0.13 and 2.46 mg m^{-3} (Fig. 5a), with the lowest values associated with the TW and SAW and the highest within the shelf and coastal waters. Concerning phytoplankton
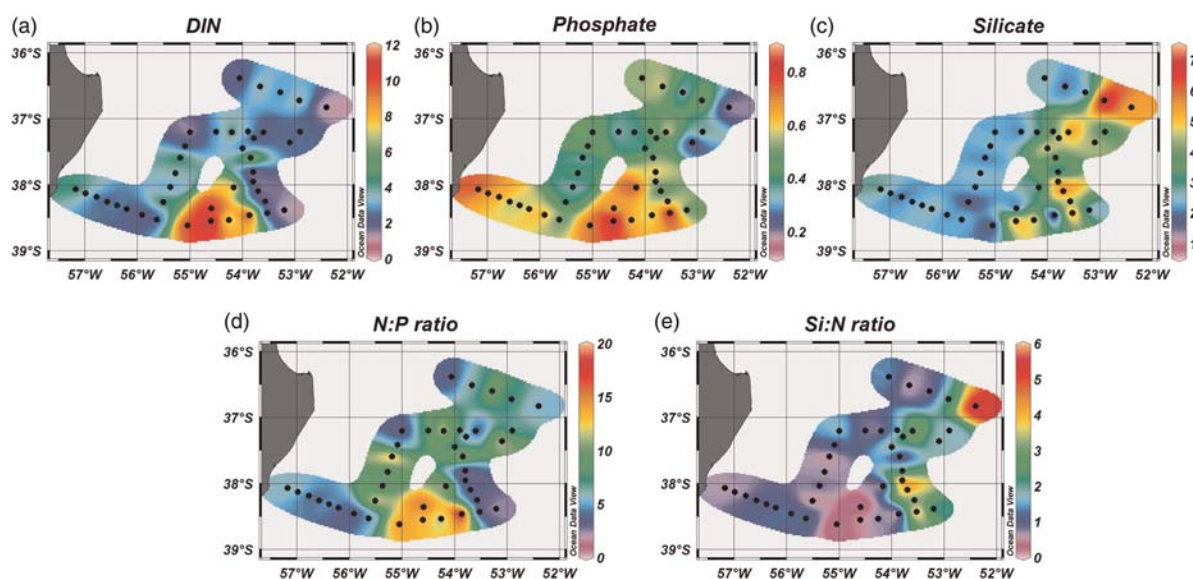
Fig. 4. Surface distribution of DIN (**a**), phosphate (**b**) and silicate (**c**), in µM, along with N:P (**d**) and Si:N (**e**) ratios in the study area.
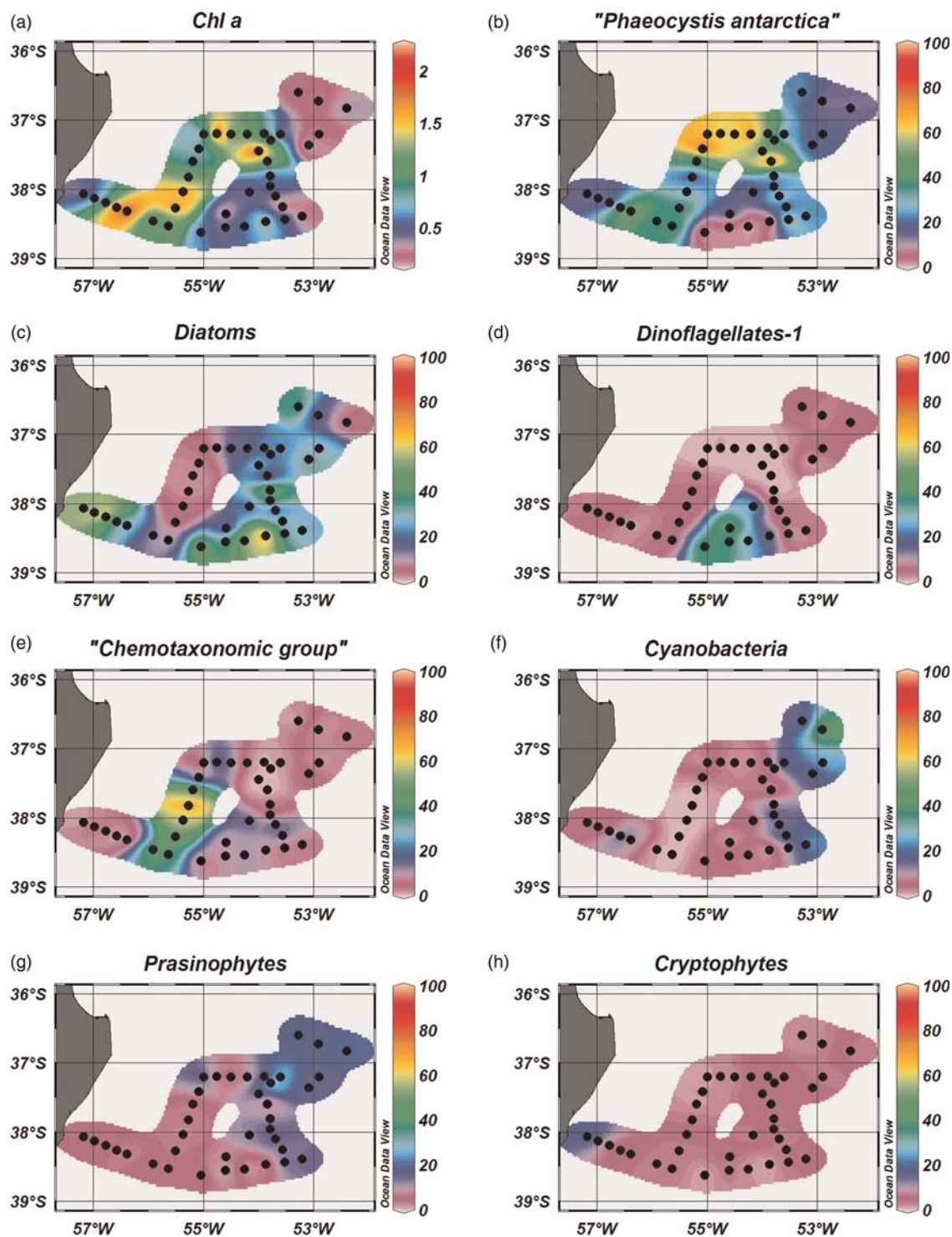
Fig. 5. Surface distributions of Chl *a* concentration (mg m^{-3}) (**a**) and relative contribution of phytoplankton groups to total Chl *a*, according to interpretation of HPLC-derived pigment data using CHEMTAX program: '*P. antarctica*' (**b**); diatoms (**c**); dinoflagellates-1 (**d**); 'Chemotaxonomic group' (**e**); cyanobacteria (**f**); prasinophytes (**g**) and cryptophytes (**h**).

distributions, the haptophyte 'Phaeocystis antarctica' was present at all stations, but was mainly associated with the shelf and mixing waters, particularly at northern stations and almost absent in the SAW (Fig 5b). Diatoms were also ubiquitous, with the highest contributions (>50%) within stations under the influence of SAW and LSCW (Fig. 5c). Additionally, diatoms showed the lowest contributions (<10%) at the shelf stations, where 'P. antarctica' was important. Dinoflagellates-1 showed high contributions (between 17 and 42%), only at stations under the influence of SAW (Fig. 5d). The highest contributions of 'chemotaxonomic group' (ranging from 38 to 68%) were found on the shelf, sharing importance with 'P. antarctica' at some stations (Fig. 5e). Cyanobacteria and prasinophytes were particularly relevant in the warmer TW, with a maximum contribution of 44 and 36%, respectively (Fig. 5f and g), but unimportant at the other stations. Cryptophytes were only noticeable at coastal stations under LSCW influence (Fig. 5h).

Results of phytoplankton microscopic analysis, including data on heterotrophic species and also on ciliates, are shown in Table III. Small Flagellates (or Flagellates I, $2-5 \mu m$), among which is the haptophyte P. antarctica (the only identifiable small flagellate during the lab routine), dominated all water masses. These organisms were present in higher concentration in the shelf and mixing waters (up to 7.7×10^6 cells L^{-1}) but high concentrations of nanoflagellates (reaching 2.9×10^6 cells L^{-1}) were also found in TW; their lowest concentrations were estimated for stations located in the SAW (between 0.05 and 0.2×10^6 cells L^{-1}) and for the coastal stations (ranging from 0.08 to 0.2×10^6 cells L^{-1}) (Table III). Significant diatom concentrations were found within the following water masses/zones: Chaetoceros spp. I ($<10 \mu m$), Thalassiosira spp. I ($<20 \mu m$) and Pseudonitzschia spp. showed higher numbers within SAW, while Cylindrotheca closterium was representative of shelf and mixing waters of the intermediate zone (IZ); Guinardia spp. and Thalassionema nitzschioides were important in TW's diatom assemblage and Asteromphalus sarcophagus, Guinardia delicatula and Rhizosolenia spp. (e.g. R. setigera) were almost exclusively found in the coastal portion of the survey area. Regarding dinoflagellates, the Sub-Antarctic Zone (SAZ) exhibited the highest abundance of auto-/mixotrophic (basically Gymnodinium spp., Ceratium lineatum/pentagonum, Peridinids and Prorocentrum minimum) and heterotrophic dinoflagellate species (Amphidinium sphenoides, Gyrodinium fusiforme and Protoperidinium spp.). Among the ciliates, a higher concentration of the autotrophic Myrionecta rubra and the presence of tintinids (Dadayiella ganymedes, Dictyocysta elegans speciosa and Salpingella spp.) were prominent within the TW, but a predominance of aloricate oligotrichids was observed across the remaining area.

Statistical analysis

Both total Chl a and relative contribution of taxonomic groups estimated by CHEMTAX showed no significant differences (based on t-tests; data not shown) between the surface and the fluorescence peak depth at most sampling stations. The only exception was at stations located under the influence of TW, where conspicuous fluorescence peaks were observed and significant differences between the surface and the fluorescence peak were found mainly for dinoflagellates and the 'chemotaxonomic group' (no microscopic data were available for those depths). Thus, only the surface phytoplankton distribution data were used in the statistical analysis for the study area description.

Cluster analysis results based on the absolute abundance of major phytoplankton groups (Fig. 6) showed four clusters, at the 0.68 similarity level (cophenetic correlation coefficient: $c = 0.92$), in reasonable agreement with the water masses distribution from the T–S diagram (Fig. 3). The four clusters displayed in Fig. 6 were used to divide the study area into four distinct zones, as follows: a coastal zone (CZ) represented by the LSCW; a SAZ including stations under the influence of SAW low temperatures; a tropical zone (TZ) represented by TW-dominated stations of high temperature and salinity values and an IZ associated with the presence of shelf waters (SASW and STSW) and mixing waters (Fig. 7 for locations of zones). Those zones could also be discriminated in the surface distribution patterns of the environmental factors (both physical and chemical). Average values of the main variables in each zone are shown in Table IV.

Results of the CCA analysis (Table V and Fig. 8) were used to investigate the association of species or higher taxonomic categories to environmental variables. A Monte-Carlo test of the F-ratio, applied during the CCA analysis, showed that the seven environmental variables (temperature, salinity, DIN, phosphate, silicate, UMLD and water column stability) contributed significantly to the observed spatial distribution of phytoplankton groups ($P < 0.01$). In fact, environmental variability explained 44% of the spatial variability in phytoplankton communities and the first two significant canonical roots cumulatively explained 73% of the observed variance. The first canonical root (which explained 47% of the variation) clearly distinguished species/groups (triangles in Fig. 8) most positively related to salinity and temperature, while the second

Table III: Checklist of main species or higher level taxa identified in surface waters during the 'PATEX VI' cruise and ranges of cell abundance (cells L^{-1}) for respective zones identified in this work

Taxonomic groups	Coastal zone	Sub-Antarctic zone	Tropical zone	Intermediate zone
Flagellates I (a, b) (2–5 μm; including *Phaeocystis antarctica*)	75 842–176 965	52 367–191 411	65 008–2 900 061	151 684–7 746 739
Flagellates II (>5 μm) (a, b)	1803–13 526	0–19 682	0–191 167	0–26 150
Class Cryptophyceae (a, b)	902–15 329	0–15 329	0–4960	0–42 381
Class Dinophyceae				
Amphidinium sphenoides		0–922		
Ceratium furca (a, b)			0–20	
Ceratium fusus (a, b)		0–40	0–20	
Ceratium lineatum/pentagonum (a, b)	0–360	0–1920	0–400	
Ceratium pentagonum (a, b)		0–620	0–40	
Ceratium tripos tripos (a, b)	20–40		0–20	0–20
Cochlodinium spp.		0–280	0–180	
Dinophysis spp. (a, b)		0–140	0–20	
Gonyaulax scrippsae (a, b)	0–100	0–380		
Gymnodinium spp. I (<20 μm) (a, b)	902–6312	6763–59 064	4960–45 988	0–14 428
Gymnodinium spp. II (>20 μm) (a, b)	0–160	2580–25 920	80–3040	0–20
Gymnodinium filum		0–40		
Gymnodinium splendens		80–22 080	0–160	0–20
Gyrodinium fusiforme		0–3520	0–40	
Gyrodinium sp. (<20 μm) (a, b)	0–902	0–2254	0–4960	
Gyrodinium spp. (>20 μm)	0–2300	520–3000	0–540	
Katodinium spp.		0–1803	0–1803	0–451
Noctiluca scintilans	20–60			
Oblea baculifera	0–20	0–40		
Oxytoxum spp. (a, b)		0–3156	0–4058	0–451
Peridiniales I (<20 μm) (a, b)	902–1803	1803–29 306	0–13 075	0–902
Peridiniales II (>20 μm) (a, b)	1011–4007	451–2400	0–1803	
Polykrikos sp.			0–140	
Prorocentrum micans (a, b)	20–460		0–120	0–20
Prorocentrum minimum (a, b)	1353–1803	2254–9468	0–7214	0–3607
Prorocentrum minimum (~ 20 μm) (a, b)	80–1420		0–60	0–20
Prorocentrum rostratum (a, b)			0–380	
Prorocentrum aff. *scutellum* (a, b)		340–1620	60–500	0–20
Protoperidinium spp.	440–780	300–8180	40–902	0–20
Scrippsiella cf. *trochoidea* (a, b)		0–200		
Torodinium robustum (a, b)	100–240	0–180	0–120	0–20
Other autotrophic dinoflagellates (a, b)	0–40	0–920	0–40	
Class Bacillariophyceae				
Asteromphalus sarcophagus (a, b)	0–2254			
Chaetoceros spp. I (<10 μm) (a, b)		0–293 965	0–22 543	
Chaetoceros spp. II (>10 μm) (a, b)	0–6312	0–14 777	0–25 051	
Cylindrotheca closterium (a, b)		0–4509	0–4058	0–115 569
Guinardia delicatula (a, b)	902–26 601		0–19 838	
Guinardia striata (a, b)			0–400	
Guinardia tubiformis (a, b)		0–902		
Guinardia spp. (a, b)	160–180	0–200	0–6843	
Hemiaulus spp. (a, b)		0–1353	0–180	
Meuniera membranaceae (a, b)	0–180			
Nitzschia cf. *longissima* (a, b)	120–902	0–120		
Pseudonitzschia spp. (a, b)	0–10 370	0–65 827	0–31 561	
Rhizosolenia spp. (a, b)	400–5280		20–620	0–20
Thalassionema nitzschioides (a, b)			0–8110	
Thalassionemataceae (a, b)		0–240	0–1500	
Thalassiosira spp. I (<20 μm) (a, b)	15 780–22 543	451–132 555	0–962	0–451
Thalassiosira spp. II (>20–50 μm) (a, b)	120–400	0–1000	0–100	0–20
Thalassiosira spp. III (>50–100 μm) (a, b)		0–20	0–60	
Other centrics (a, b)	6332–20 289	0–160	0–1353	0–5417
Other pennates (a, b)	0–300	0–200	20–1453	
Ciliophora				
Didinium spp.		0–1140	0–40	0–40
Monodinium sp.			0–80	
Lacrymaria sp.		0–80		
Myrionecta rubra (a, b)	200–831	0–360	0–5169	0–902
Dadayiella ganymedes			0–220	

Continued

Table III: Continued

Taxonomic groups	Coastal zone	Sub-Antarctic zone	Tropical zone	Intermediate zone
Dictyocysta elegans speciosa			0–40	
Salpingella spp.		0–40	0–140	
Laboea strobila	0–160	0–20	0–20	0–20
Strobilidium spp.	180–200	80–480	40–320	0–20
Strombidium spp.	60–120	20–600	120–500	0–40
Tontonia gracilima		0–40	0–20	
Vorticelids		0–520	0–20	
Oligotrichids (<20 μm)	60–260	451–3847	1353–6312	0–902
Other ciliates		0–200	0–20	

The autotrophic organisms were labeled (a) and those used in the cluster and canonical correspondence analysis were labeled (b).
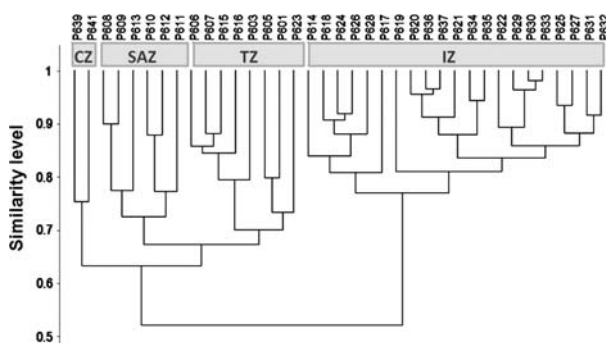

Fig. 6. Dendrogram for sampling stations based on absolute abundance of major phytoplankton groups at the surface [less frequent taxa (<10%) were excluded] from microscopic analysis, using Bray–Curtis similarity index and group average linkage. The clusters were named according to four similarity zones as follows: coastal zone (CZ), Sub-Antarctic Zone (SAZ), tropical zone (TZ) and intermediate zone (IZ).

(26%) suggested that the species/groups were more related to temperature (negatively) and to DIN and phosphate (positively) (see the factor loadings in Table V and Fig. 8). Ordination of the samples in the first two canonical roots shows a clear separation of the TZ, SAZ, IZ and (not so clearly) CZ stations (Fig. 8), which were distributed in direct relation to the surface water masses distribution. Since distance between stations in the ordination diagram corresponds to the level of similarity among stations (ter Braak, 1994), the second canonical root can be interpreted as indicating a gradual change in phytoplankton structure from the Tropical to the SAZs, with high variability associated with the CZ stations. In addition, there is also a high variability within the TZ and SAZs along the first canonical root. This possibly represents the large spatial variability found in phytoplankton abundance and community composition within the survey area, as noted in the cluster analysis (Fig. 6) and seen in the mosaic-like spatial structure of the zones (Fig. 7).

The high factor loadings found when associated with temperature and salinity (Table V; Fig. 8) reflect the strong connection between phytoplankton variability and water mass distribution. High factor loadings were also observed for the dissolved inorganic nutrients (mainly DIN and phosphate). This corroborates the hypothesis that water masses influence phytoplankton variability, since dissolved macronutrients are known as non-conservative properties of water masses and can be used to characterize some of them (Niencheski and Fillmann, 1997).

Regarding phytoplankton taxa, small (<20 um) diatoms (*Thalassiosira* spp. and *Chaetoceros* spp., and the pennate *Nitzschia* cf. *longissima*) and large (>20 um) dinoflagellates (*Gymnodinium* spp., *Ceratium* spp., *Gonyaulax* cf. *scrippsae*) were more associated with the SAZ. Conversely, cyanobacteria, other diatoms (e.g. *Hemiaulus* spp., *Rhizosolenia* spp., *Guinardia delicatula*, *Thalassionema nitzschioides*) and the dinoflagellate *Prorocentrum rostratum* were strongly related to the TZ (Fig. 8). Within the IZ, an assemblage of Flagellates was important (comprising a wide size spectrum, from 2 to 10 μm in length) that included FlagI (mostly the haptophyte *Phaeocystis antarctica*), FlagII and cryptophytes. The dinoflagellates *Prorocentrum minimum* and *P. micans* and the nano-pennate diatom *Cylindrotheca closterium* were also found in that zone. The CZ did not show a marked pattern, but was characterized by some unique diatoms (e.g. *Asteromphalus sarcophagus*) and neritic dinoflagellates.

DISCUSSION

Several studies have described the spatial phytoplankton distribution based on *in situ* data (Carreto *et al.*, 1995, 2003, 2008; Brandini *et al.*, 2000; Olguín *et al.*, 2006) as well as on the variability of phytoplankton biomass and primary production based on satellite images, near the BMC region (Garcia *et al.*, 2004; González-Silvera *et al.*, 2006; Romero *et al.*, 2006; Lutz *et al.*, 2010). This area has also been identified as having conspicuous
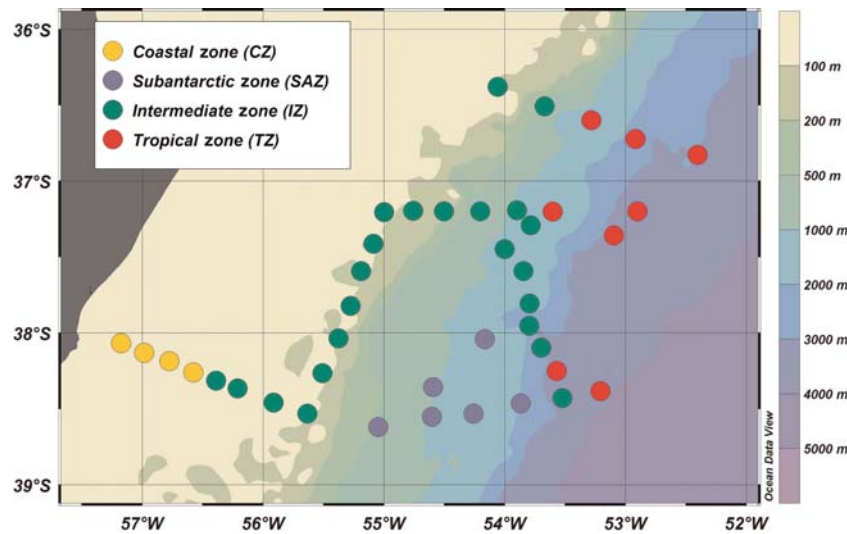
Fig. 7. Schematic map of the four zones classified based on phytoplankton distribution. Inset shows the labels for the respective zones and color bar indicates isobaths (m).

Table IV: Mean and minimum−maximum values of environmental variables at the surface (or water column for UMLD and stability) for each zone within the study region, discriminated by the Cluster analysis

	CZ	SAZ	TZ	IZ
Temperature (°C)	12.7 (11.7−13.7)	8.4 (8.1−8.7)	17.6 (16.9−18.8)	11.4 (9.9−13.9)
Salinity	33.69 (33.47−33.91)	33.92 (33.85−34.02)	34.75 (33.84−35.98)	33.62 (33.04−33.89)
Chl *a* (mg m^{-3})	0.92 (0.29−1.98)	0.53 (0.30−0.90)	0.22 (0.13−0.36)	1.11 (0.39−2.27)
DIN (μM)	3.22 (1.88−4.67)	9.22 (6.52−10.92)	2.04 (0.94−3.62)	2.78 (1.24−6.64)
Phospahte (μM)	0.66 (0.53−0.79)	0.66 (0.55−0.76)	0.40 (0.18−0.63)	0.48 (0.34−0.89)
Silicate (μM)	2.33 (1.53−3.15)	2.27 (0.61−5.18)	4.35 (1.83−7.33)	3.14 (1.69−6.41)
N:P	4.8 (3.5−6.3)	14.3 (10.7−19.8)	5.9 (2.3−11.8)	6.4 (1.5−14.0)
Si:N	0.8 (0.5−1.3)	0.3 (0.06−0.8)	2.5 (0.7−5.7)	1.6 (0.4−4.8)
UMLD (m)	15 (9−25)	9 (8−13)	14 (8−20)	12 (7−20)
Stability (10^{-8} rad^2 m^{-1})	1153.2 (893.2−1716.1)	885.1 (611.1−1085.9)	1392.7 (318.2−2622.7)	1846.9 (1129.2−4421.2)
DegP: Chl *a*	0.017 (0.006−0.025)	0.046 (0.016−0.074)	0.011 (0−0.028)	0.03 (0.006−0.078)

DegP, degradation products of Chl *a* (chlorophyllide *a*, pheophytin *a* and pheophorbide *a*).

Table V: Factor loadings (correlation coefficients) of environmental variables with canonical roots estimated by canonical correspondence analysis in Fig 7

Parameter	First canonical root	Second canonical root
Temperature	0.445	−0.780
Salinity	0.634	−0.363
DIN	0.173	0.873
Phosphate	−0.039	0.571
Silicate	−0.008	−0.350
UMLD	−0.369	−0.350
Stability	0.201	−0.459

biological gradients in which subtropical and Sub-Antarctic plankton species are found (e.g. Boltovskoy, 1981). In the present work, four zones were identified in the study area, based on phytoplankton distribution and these were clearly discriminated according to physical features (conservative and non-conservative properties of water masses). In the eastern section, the TZ was influenced only by TW, although the influence of BC was also observed in the northeastern part of the IZ, dominated by STSW. A similar classification scheme has also been adopted in other investigations over and/ or near this region (Carreto *et al.*, 2003, 2008), including a wider coverage of coastal and estuarine areas. Nonetheless, the authors did not identify the STSW along the continental shelf, since their sampling sites were located further south in comparison with our sampling grid, which covered the northernmost shelf sites in the Argentine Sea. Additionally, a stronger thermal gradient (0.173°C km^{-1}) found between the TZ and SAZ

Fig. 8. Canonical correspondence analysis ordination diagram relative to data on surface abundance of phytoplankton [less frequent taxa (<10%) were excluded] data. The first two significant canonical roots represent 73% of phytoplankton groups–environment relationships. Arrows refer to environmental variables. Sampling stations (where all data were available) are represented by colored circles, according to identified zones (as in Fig. 7). Triangles refer to surface absolute abundance of major species/groups, whose abbreviations are as follows: Flagellates I (2–5 μm; including *Phaeocystis antarctica*—FlagI), Flagellates II (>5 μm—FlagII), Class Cryptophyceae (Crypt), *Ceratium* spp. (Cer), *Cochlodinium* sp. (Coch), *Dinophysis* spp. (Dinph), *Gonyaulax* cf. *scrippsae* (Gony), *Gymnodinium* spp. I (<20 μm—GymnI), *Gymnodinium* spp. II (>20 μm - GymnII), *Gyrodinium* sp. I (<20 μm—GyroI), *Oxytoxum* spp. (Oxyt), Peridiniales I (<20 μm—PerI), Peridiniales II (>20 μm—PerII), *Prorocentrum micans* (Pmic), *P. minimum* (Pmin), *P. minimum* II (~20 μm—PminII), *P. rostratum* (Prost), *P.* aff. *scutellum* (Pscut), *Scrippsiella* cf. *trochoidea* (Scripp), *Torodinium robustum* (Torod), other dinoflagellates (Dinof), *Asteromphalus sarcophagus* (Asarco), *Chaetoceros* spp. I (<10 μm—ChaetI), *Chaetoceros* spp. II (>10 μm—ChaetII), *Cylindrotheca closterium* (Cylclo), *Guinardia delicatula* (Gdelic), *Guinardia* spp. (Gspp), *Hemiaulus* spp. (Hspp), *Meuniera membranaceae* (Mmembr), *Nitzschia* cf. *longissima* (Nlong), *Pseudonitzschia* spp. (Pseudo), *Rhizosolenia* spp. (Rhizo), *Thalassionema nitzschioides* (Tnitz), *Thalassionemataceae* (Tnema), *Thalassiosira* spp. I (<20 μm—ThaI), *Thalassiosira* spp. II (>20–50 μm—ThaII), *Thalassiosira* spp. III (>50–100 μm—ThaIII), other centrics (Centr), other pennates (Penn), *Myrionecta rubra* (Mrub).

was computed in our study when compared with other front studies with values of 0.065, 0.1 and 0.144°C km^{-1} (Bianchi *et al.*, 1993; Souza and Robinson, 2004; Berasategui *et al.*, 2005, respectively). This highlights the strong physical barrier established between the TW and SAW sub-domains during our study period.

Regarding the nutrient distribution pattern, a marked reflection of the physical zonation was observed: the highest N and P concentrations (up to 11.62 μM of DIN and 0.89 μM of phosphate) were determined in the SAZ, while the highest (maximum of 7.33 μM) silicate level was determined in the TZ. Relatively higher silicate levels have been attributed to TW (with values

>4 μM) in relation to nitrogen and phosphate in the southern Brazilian shelf (Niencheski and Fillmann, 1997). Intermediate values of all nutrients were found in both the Intermediate and CZ (except for phosphate in the CZ; Fig. 4). Similar patterns of nutrient distributions have been found close to the region, with high nitrogen and phosphate associated with SAW (SAZ) in contrast to oligotrophic TW (Brandini *et al.*, 2000; Painter *et al.*, 2010). The silicate-rich TW observed in our study are in contrast to low silicate levels within the SAW (SAZ) as previously observed (Garcia *et al.*, 2008). Consequently, average N:P values close to Redfield (14.3) and low (0.3) average Si:N ratios were found in the SAZ, suggesting a phytoplankton community under a progressive Si

limitation (Egge and Aksnes, 1992). On the other hand, low (5.9) N:P and high (2.5) Si:N in the TZ could indicate an N-limited phytoplankton community (e.g. Barlow *et al.*, 2002). However, phytoplankton growth has been demonstrated to occur over a wide range of N:P ratios, ranging from 5 to 34 (Geider and La Roche, 2002). The wide range of environmental N:P ratios in which phytoplankton can grow is a reflection of the highly variable elemental stoichiometry of marine phytoplankton species/groups (e.g. Ho *et al.*, 2003; Quigg *et al.*, 2003; Klausmeier *et al.*, 2004a; Arrigo, 2005). This variability is determined by the particular nutrient requirements of each species/group and the flexibility in their overall stoichiometry, often matching their nutrient supply at low growth rates (Rhee, 1978; Klausmeier *et al.*, 2004b). Laboratory studies have shown that the canonical Redfield N:P ratio of 16 is not a universal biochemical optimum, but instead represents an average of species-specific N:P ratios (e.g. Klausmeier *et al.*, 2004a). Finally, in the IZ and CZ there was not a clear indication of a particular nutrient limitation, based on nutrient ratios.

Many studies on phytoplankton growth have shown that, in most frontal zones, phytoplankton blooms are generally distributed along narrow bands (Laubsher *et al.*, 1993; Olson *et al.*, 1994; Longhurst, 1998). However, the BMC region represents a large-scale phenomenon with a vast area of relatively high phytoplankton biomass, due to the extensive frontal zone generated by the confluence of the BC and the MC (Brandini *et al.*, 2000; Barré *et al.*, 2006). In our study, higher Chl *a* concentrations (≥ 1 mg m^{-3}) were observed across the IZ and CZ (Table IV), including both shelf and mixing waters (between the BC and the MC). This pattern has also been observed during springtime, where highest Chl *a* concentrations were found associated with a coastal front close to our southernmost cross-shelf transect (Carreto *et al.*, 1995).

The occurrence of major phytoplankton groups, determined from the CHEMTAX analysis, within the study region, can be summarized as follows: diatoms, '*Phaeocystis antarctica*' and 'chemotaxonomic group' were more frequent than dinoflagellates-1, prasinophytes, cyanobacteria and cryptophytes over the whole study area. The patchy distribution of those groups closely reflected the physical zonation identified in this study. The set of abiotic factors was reasonably informative (44% of variation explained) of the spatial variability in phytoplankton communities. Salinity and temperature showed the highest correlations with the first canonical root (see CCA in Fig. 8), indicating the importance of the water mass signal on the spatial distribution of species within the BMC, mainly through the influence

on nutrient supply. In fact, nutrients (basically DIN and phosphate) were major factors affecting the phytoplankton community, particularly within the colder SAW, as displayed in the second canonical root. Water column stability and silicate showed lower and negative correlations with this canonical root and were mostly associated with stations in the IZ (Fig. 8). UMLD showed similar (but opposing) correlations with the two significant canonical roots, denoting its less important influence on phytoplankton variability in this study (Table V).

The SAZ was characterized by relatively low values of temperature, stability, silicate and UMLD, but high DIN and phosphate as well as moderate Chl *a* concentrations (Table IV). In this zone, many species of dinoflagellates and diatoms were the main phytoplankton organisms. The predominance of SAW-related diatoms has already been described near our SAZ [e.g. many small ($<$10 μm) *Chaetoceros* spp.] (Fernandes and Brandini, 1999; Olguín *et al.*, 2006). Garcia *et al.* (Garcia *et al.*, 2008) found a remarkable bloom composed mainly of diatoms and dinoflagellates further south, along the Patagonia shelf-break front. However, low phytoplankton biomass and high macronutrient levels were found on the eastern side of that front, associated with typical MC waters and a deeper UMLD. A different phytoplankton community, mainly composed of very small Flagellates (particularly *Phaeocystis* sp.), dominated the area under those conditions. In the present study, the SAZ under the influence of SAW exhibited high concentrations of nitrogen coupled with a shallow UMLD, which might have favored phytoplankton growth. However, Chl *a* levels were not particularly high and this is probably due to loss processes through grazing. This is suggested by the comparatively higher abundances of potential grazers such as mixotrophic/ heterotrophic dinoflagellates (large *Gyrodinium* spp.) and ciliates such as *Didinium* spp., *Strombilidium* spp. and *Strombidium* spp. in this zone (Table III). Mixotrophic/ heterotrophic dinoflagellate dominance has already been reported in SAW closer to the BMC region with a contribution of *Gyrodinium* spp. together with large autotrophic species, such as *Ceratium lineatum*, *C. pentagonum grande*, *Dinophysis okamurai*, *Gymnodinium* spp. and *Prorocentrum* sp. (Fernandes and Brandini, 1999). The dominance of dinoflagellates along the SAZ could be related to possible Si limitation of diatom growth (mean Si:N = 0.3) in this area (Table IV).

On the eastern side of the study area, the TZ was represented by high values of silicate concentrations, temperature and salinity coupled with low DIN, phosphate and Chl *a* concentrations, on average (Table IV). This combination of factors seemed to favor a

significant contribution of cyanobacteria and prasino-phytes (determined by CHEMTAX) and of other distinct diatoms, such as *Hemiaulus* spp. and *Thalassionema nitzschioides*. Again, those diatoms have been found before in sub-tropical waters (Gayoso and Podestá, 1996; Fernandes and Brandini, 1999; Olguín *et al.*, 2006) as well as cyanobacteria and small Flagellates, which were usually abundant within the BC (Fernandes and Brandini, 1999; Carreto *et al.*, 2008). The dominance of cyanobacteria in sub-tropical waters was also observed along the geostrophic front in the Eastern Alboran Sea (Claustre *et al.*, 1994), while a dominance of cryptophytes and prasinophytes (in 2000 and 2001, respectively) was found in eastern New Zealand waters (Delizo *et al.*, 2007). In oligotrophic waters, such small cells (particularly prokaryotes) thrive because they have low requirements for nutrients when compared with larger cells (Whitfield, 2001). However, the presence of relatively large diatoms in the TW in this work is fairly unexpected, taking into account the relatively low nutrient concentrations (mainly DIN and phosphate), since diatoms are poor competitors at low phosphate concentrations (Egge, 1998).

Stations located in the IZ represented a transition between the two sub-domains (SAZ and TZ) of contrasting characteristics (Table IV). Besides the important presence of the small-sized pennate diatom *Cylindrotheca closterium* and the dinoflagellates *Prorocentrum minimum* and *Gymnodinium* spp. (<20 µm), mainly small Flagellates dominated over this region, grouped as 'chemotaxonomic group' (Fig. 6). Among those Flagellates, *Phaeocystis antarctica* was dominant at most sites and, generally, under the influence of SAWs. This haptophyte has been previously observed in SAWs of the MC, while other haptophytes were associated with a continental shelf community (Carreto *et al.*, 2003). In our study, besides *P. antarctica*, other nanoflagellates (FlagI and FlagII determined by microscopic observations) probably included coccolithophores and chrysophytes, as previously observed along the shelf-break (Carreto *et al.*, 2003), but not clearly identified in our study either by microscopy or by CHEMTAX. A similar pattern of enhanced Chl *a* concentration along the frontal (mixing) zone was found in studies developed in the Eastern Alboran Sea (Claustre *et al.*, 1994) and along the subtropical convergence east of New Zealand (Delizo *et al.*, 2007); however, both studies have detected a diatom dominance associated with those high Chl *a* zones in contrast to the pattern of *Phaeocystis antarctica* dominance found in our study.

The CZ was marked by moderate temperature and low salinity, probably due to dilution by continental waters. Also, high phosphate levels and a deeper UMLD were found within this zone. Although the phytoplankton community was similar to the IZ, it included some typical neritic dinoflagellates such as *Noctiluca scintillans* and *Ceratium tripos*, previously described by Balech (Balech, 1988).

Apart from the physical and chemical factors controlling the development and distribution of phytoplankton communities, the role of microzooplankton (ciliates and heterotrophic dinoflagellates) and mesozooplankton (e.g. copepods) grazing on phytoplankton blooms has to be considered. This has been mentioned particularly for the SAW, across the Argentine Sea, when fast growth of primary producers in spring and summer was associated with high abundances of grazers such as copepods (Sabatini *et al.*, 2004). Ammonium concentration can be an indicator of grazing pressure, since it is a common excretion product derived from heterotrophic metabolism (e.g. Pernthaler, 2005). High levels of ammonium along the Patagonian shelf-break were suggested as an indication of grazing pressure controlling the phytoplankton biomass (Garcia *et al.*, 2008; Painter *et al.*, 2010). In the present study, ammonium reached up to 50% of surface DIN, mainly within the IZ and TZ, while the lowest ammonium proportions were observed in the CZ ($13-24\%$) and SAZ ($1-7\%$) (data not shown). At the same time, a higher proportion of Chl *a* degradation products, which are usually associated with grazing processes, was found in the SAZ, compared with the other zones (Table IV), but it was only statistically different from the average proportion of the TZ (Kruskal–Wallis test H, $P < 0.05$). In fact, a rich zooplankton community, including mesozooplankton groups, has been shown to occur at the BMC region (Berasategui *et al.*, 2005). It is possible that in the SAW there was a tight coupling between the growth of phytoplankton, based on consumption of ammonium and other nutrients, and a concurrent high grazing pressure, constraining the accumulation of the phytoplankton biomass (average 0.53 mg m^{-3}) in the SAZ.

CONCLUSION

The BMC region studied in this work shows a complex distribution of phytoplankton communities, due to environmental forcing. High Chl *a* was associated with shelf and mixed waters, under strong water column stability and moderate nutrient concentration, favoring mainly the growth of *Phaeocystis antarctica*. Coastal waters showed moderate Chl *a* associated with the presence of typical neritic dinoflagellate species and a deep UMLD. Tropical and SAWs showed relatively low Chl *a*, related to low nutrient levels (N and P) and strong stability

(tropical) and Si limitation (Sub-Antarctic). The patchy distribution of phytoplankton communities mainly followed the water mass distribution in the study region. These results emphasize the importance of both conservative and non-conservative properties of water masses for the structure of phytoplankton communities.

REFERENCES

Aminot, A. and Chaussepied, J. (1983) *Manuel dês Analyses Chimiques en Milieu Marin*. C.N.E.X.O, Brest, 230 pp.

Arrigo, K. R. (2005) Marine microorganisms and global nutrient cycles. *Nature*, **437**, 349–355.

Balech, E. (1988) Los dinoflagelados del Atlantico Sudoccidental. *Publ. Espec. Inst. Esp. Oceanogr.*, **1**, 1–310. Madrid.

Barlow, R. G., Aiken, J., Holligan, P. M. *et al.* (2002) Phytoplankton pigment and absorption characteristics along meridional transects in the Atlantic Ocean. *Deep-Sea Res. I.*, **47**, 637–660.

Barré, N., Provost, C. and Saraceno, M. (2006) Spatial and temporal scales of the Brazil-Malvinas Current confluence documented by simultaneous MODIS Aqua 1.1-km resolution SST and color images. *Adv. Space Res.*, **37**, 770–786.

Berasategui, A. D., Ramírez, F. C. and Schiariti, A. (2005) Patterns in diversity and community structure of epipelagic copepods from the Brazil-Malvinas Confluence area, south-western Atlantic. *J. Marine Syst.*, **56**, 309–316.

Bianchi, A. A., Bianucci, L., Piola, A. R. *et al.* (2005) Vertical stratification and air-sea CO2 fluxes in the Patagonian shelf. *J. Geophys. Res.*, **110**, 1–10.

Bianchi, A. A., Giulivi, C. F. and Piola, A. R. (1993) Mixing in the Brazil-Malvinas Confluence. *Deep-Sea Res. I*, **40**, 1345–1358.

Bianchi, A. A., Piola, A. R. and Collino, G. J. (2002) Evidence of double diffusion in the Brazil-Malvinas *Confluence. Deep- Sea Res. I*, **49**, 41–52.

Boltovskoy, D. (1981) Características biológicas del Atlántico Sudoccidental. In Boltovskoy, D. (ed.), *Atlas del Zooplancton del Atlantico Sudoccidental y Métodos de Trabajo con el Zooplancton Marino*. INIDEP, Mar del Plata, pp. 239–251.

Brandini, F. P., Boltovskoy, D., Piola, A. *et al.* (2000) Multiannual trends in fronts and distribution of nutrients and chlorophyll in the southwestern Atlantic (30–62°S). *Deep-Sea Res. I*, **47**, 1015–1033.

Campagna, C., Piola, A. R., Marin, M. R. *et al.* (2006) Southern elephant Seal trajectories, fronts and eddies in the Brazil/Malvinas Confluence. *Deep-Sea Res. I*, **53**, 1907–1924.

Carreto, J. I., Lutz, V. A., Carignan, M. O. *et al.* (1995) Hydrography and chlorophyll *a* in a transect from the coast to the shelf-break in the Argentinean Sea. *Cont. Shelf Res.*, **15**, 315–336.

Carreto, J. I., Montoya, N., Akselman, R. *et al.* (2008) Algal pigments patterns and phytoplankton assemblages in different water masses of the Río de la Plata maritime front. *Cont. Shelf Res.*, **28**, 1589–1606.

Carreto, J. I., Montoya, N. G., Benavides, H. R. *et al.* (2003) Characterization of spring phytoplankton communities in the Río de La Plata maritime front using pigment signatures and cell microscopy. *Mar. Biol.*, **143**, 1013–1027.

Chelton, D. B., Schlax, M. G., Witter, D. L. *et al.* (1990) Geosat altimeter observations of the surface circulation of the Southern Ocean. *J. Geophys. Res.*, **95**, 17877–17903.

Clarke, K. R. and Warwick, R. M. (1994) *Changes in Marine Communities: An Approach to Statistical Analysis and Interpretation*. Natural Environmental Research Council, Plymouth, UK, 234 pp.

Claustre, H., Kerhervé, P., Marty, J. C. *et al.* (1994) Phytoplankton dynamics with a geostrophic front: ecological and biogeochemical implications. *J. Mar. Res.*, **52**, 711–742.

Delizo, L., Smith, W. O. and Hall, J. (2007) Taxonomic composition and growth rates of phytoplankton assemblages at the Subtropical Convergence east of New Zealand. *J. Plankton Res.*, **29**, 655–670.

de Souza, M. S., Mendes, C. R. B., Garcia, V. M. T. *et al.* (2011) Phytoplankton community during a coccolithophorid Bloom in the Patagonian shelf: microscopic and high-performance liquid chromatography pigment analyses. *J. Mar. Biol. Assoc.*, **92**, 13–27.

Dodge, J. D. (1982) *Marine Dinoflagellates of the British Isles*. Her Majesty's Stationary Office, London.

Egge, J. K. (1998) Are diatoms poor competitors at low phosphate concentrations? *J. Marine Syst.*, **16**, 191–198.

Egge, J. K. and Aksnes, D. L. (1992) Silicate as regulating nutrient in phytoplankton competition. *Mar. Ecol.-Prog. Ser.*, **83**, 281–289.

Fernandes, L. F. and Brandini, F. P. (1999) Comunidade microplanctônica no Oceano Atlântico Sul Ocidental: biomassa e distribuição em novembro de 1992. *Rev. bras. oceanogr.*, **47**, 189–205.

Garcia, C. A. E., Sarma, Y. V. B., Mata, M. M. *et al.* (2004) Chlorophyll variability and eddies in the Brazil-Malvinas Confluence region. *Deep-Sea Res. II*, **51**, 159–172.

Garcia, V. M. T., Garcia, C. A. E., Mata, M. M. *et al.* (2008) Environmental factors controlling the phytoplankton blooms at the Patagonia shelf-break in spring. *Deep-Sea Res. I*, **55**, 1150–1166.

Gayoso, A. M. and Podestá, G. P. (1996) Surface hydrography and phytoplankton of the Brazil-Malvinas currents confluence. *J. Plankton Res.*, **18**, 941–951.

Geider, R. J. and La Roche, J. (2002) Redfield revisited: variability of C:N:P in marine microalgae and its biochemical basis. *Eur. J. Phycol.*, **37**, 1–17.

Gonzalez-Silvera, A., Santamaria-del-Angel, E. and Millán-Núñez, R. (2006) Spatial and temporal variability of the Brazil-Malvinas Confluence and the La Plata Plume as seen by SeaWiFS and AVHRR imagery. *J. Geophys. Res.*, **11**, C06010, doi:10.1029/2004JC002745.

Gordon, A. L. (1989) Brazil-Malvinas Confluence—1984. *Deep-Sea Res.*, **36**, 359–384.

Hasle, G. R. and Syvertsen, E. E. (1996) Marine diatoms. In Tomas, C. R. (ed.), *Identifying Marine Diatoms and Dinoflagellates*. Academic Press Inc., London, pp. 5–385.

Ho, T., Quigg, A., Finkel, Z. V. *et al.* (2003) The elemental composition of some marine phytoplankton. *J. Phycol.*, **39**, 1145–1159.

Klausmeier, C. A., Litchman, E., Daufresne, T. *et al.* (2004a) Optimal nitrogen-to-phophorus stoichiometry of phytoplankton. *Nature*, **429**, 171–174.

Klausmeier, C. A., Litchman, E. and Levin, S. A. (2004b) Phytoplankton growth and stoichiometry under multiple nutrient limitation. *Limnol. Oceanogr.*, **49**, 1463–1470.

Koroleff, F. (1969) Direct determination of ammonia in natural waters as indophenols blue. ICES C.M. 1969/C: 9. *Hydrology Communication*, 4 p.

Laubsher, R. K., Perissinoto, R. and McQuaid, C. D. (1993) Phytoplankton production and biomass at frontal zones in the Atlantic sector of the Southern Ocean. *Polar Biol.*, **13**, 471–481.

Longhurst, A. (1998) *The Ecological Geography of the Sea*. Academic Press, Elsevier, Amsterdam, New York, 424 pp.

Lutz, V. A., Segura, V., Dogliotti, A. I. *et al.* (2010) Primary production in the Argentine Sea during spring estimated by field and satellite models. *J. Plankton Res.*, **32**, 181–195.

Mackey, M. D., Mackey, D. J., Higgins, H. W. *et al.* (1996) CHEMTAX—a program for estimating class abundances from chemical markers: application to HPLC measurements of phytoplankton. *Mar. Ecol.-Prog. Ser.*, **144**, 265–283.

Matano, R. P. (1993) On the separation of the Brazil current from the coast. *J. Phys. Oceanogr.*, **23**, 79–90.

Matano, R. P., Palma, E. D. and Piola, A. R. (2010) The influence of the Brazil and Malvinas currents on the southwestern Atlantic shelf circulation. *Ocean Sci. Discuss.*, **7**, 837–871.

Mendes, C. R., Cartaxana, P. and Brotas, V. (2007) HPLC determination of phytoplankton and microphytobentos pigments: comparing resolution and sensitivity of a C_{18} and a C_8 method. *Limnol. Oceanogr.: Methods*, **5**, 363–370.

Mitchell, B. G. and Holm-Hansen, O. (1991) Observations and modelling of the Antarctic phytoplankton crop in relation to mixing depth. *Deep-Sea Res. II*, **38**, 981–1007.

Möller, O. O., Piola, A. R., Freitas, A. C. *et al.* (2008) The effects of river discharge and seasonal winds on the shelf off southeastern South America. *Cont. Shelf Res.*, **28**, 1607–1624.

Niencheski, L. F. and Fillmann, G. (1997) Chemical characteristics. In Seeliger, U., Odebrecht, C. and Castello, J. P. (eds), *Subtropical Convergence Environments: The Coast and Sea in the Southwestern Atlantic*. Springer-Verlag, Berlin, Heidelberg, pp. 96–98.

Olguín, H. F., Boltovskoy, D., Lange, C. B. *et al.* (2006) Distribution of spring phytoplankton (mainly diatoms) in the upper 50 m of the Southwestern Atlantic Ocean (30–61°S). *J. Plankton Res.*, **28**, 1107–1128.

Olson, D. B., Hitchcok, G. L., Mariano, A. J. *et al.* (1994) Life on the edge: marine life and fronts. *Oceanography*, **7**, 52–60.

Painter, S. C., Poulton, A. J., Allen, J. T. *et al.* (2010) The COPAS'08 expedition to the Patagonian shelf: physical and environmental conditions during the 2008 coccolithophore bloom. *Cont. Shelf Res.*, **30**, 1907–1923.

Pernthaler, J. (2005) Predation on prokaryotes in the water column and its ecological implications. *Nat. Rev. Microbiol.*, **3**, 537–546.

Peterson, R. G. and Stramma, L. (1991) Upper-level circulation in the South Atlantic Ocean. *Prog. Oceanogr.*, **26**, 11044–11054.

Pezzi, L. P., Souza, R. B., Acevedo, O. *et al.* (2009) Multiyear measurements of the oceanic and atmospheric boundary layers at the Brazil-Malvinas confluence region. *J. Geophys. Res.*, **114**, D19103, doi:10.1029/2008JD011379.

Pezzi, L. P., Souza, R. B., Dourado, M. S. *et al.* (2005) Ocean-atmosphere *in situ* observations at the Brazil-Malvinas Confluence region. *Geophys. Res. Lett.*, **32**, L22603, doi:10.1029/2005GL023866.

Provost, C., Garçon, V. and Falcon, L. M. (1996) Hydrographic conditions in the surface layers over the slope-open ocean transition area near the Brazil-Malvinas Confluence during austral summer 1990. *Cont. Shelf Res.*, **16**, 215–235.

Quigg, A., Finkel, Z. V., Irwin, A. J. *et al.* (2003) The evolutionary inheritance of elemental stoichiometry in marine phytoplankton. *Nature*, **425**, 291–294.

Rhee, G.-Y. (1978) Effects of N:P atomic ratios and nitrate limitation on algal growth, cell composition and nitrate uptake. *Limnol. Oceanogr.*, **23**, 10–25.

Romero, S. I., Piola, A. R., Charo, M. *et al.* (2006) Chlorophyll-a variability off Patagonia based on SeaWiFS data. *J. Geophys. Res.*, **111**, C05021, doi: 10.1029/2005JC003244.

Sabatini, M., Reta, R. and Matano, R. (2004) Circulation and zooplankton biomass distribution over the southern Patagonian shelf during late summer. *Cont. Shelf Res.*, **24**, 1359–1373.

Sournia, A. (ed.) (1978) *Phytoplankton Manual*. UNESCO, Muséum National d'Histoire Naturelle, Paris, 337 pp.

Souza, R. B. and Robinson, I. S. (2004) Satellite and Lagrangian observations of the Brazilian Coastal Current. *Cont. Shelf Res.*, **24**, 241–262.

Stramma, L. and England, M. (1999) On the water masses and mean circulation of the South Atlantic Ocean, *J.Geophys. Res.*, **104**, 20863–20883.

ter Braak, C. J. F. (1994) Canonical community ordination. Part I. Basic theory and linear methods. *Ecoscience*, **1**, 127–140.

ter Braak, C. J. F. and Prentice, I. C. (1988) A theory of gradient analysis. *Adv. Ecol. Res.*, **18**, 271–317.

Utermöhl, H. (1958) Zur Vervollkommnung der quantitativen Phytoplankton-Methodik. *Mitt. Int. Ver. Limnol.*, **9**, 1–38.

Whitfield, M. (2001) Interactions between phytoplankton and trace metal in the ocean. *Adv. Mar. Biol*, **41**, 1–128.

Wright, S. W., Ishikawa, A., Marchant, H. J. *et al.* (2009) Composition and significance of picophytoplankton in Antarctic waters. *Polar Biol.*, **32**, 797–808.

Wright, S. W. and Jeffrey, S. W. (2006) Pigment markers for phytoplankton production. In Volkmann, J. K. (ed.), *Marine Organic Matter: Biomarkers, Isotopes and DNA*. Springer-Verlag, Berlin, Heidelberg, pp. 71–104 [The Handbook of Environmental Chemistry, Vol. 2, Part 2N].

Zapata, M., Rodríguez, F. and Garrido, J. L. (2000) Separation of chlorophylls and carotenoids from marine phytoplankton: a new HPLC method using a reversed phase C8 column and pyridine-containing mobile phases. *Mar. Ecol.-Prog. Ser.*, **195**, 29–45.

Zar, J. H. (1999) *Biostatistical Analysis*. Simon and Schuster, New Jersey, 663 pp.